

Kinetics and Dynamics of Loops, α -Helices, β -Hairpins, and Fast-Folding Proteins

WILLIAM A. EATON,* VICTOR MUÑOZ,
PEGGY A. THOMPSON, ERIC R. HENRY, AND
JAMES HOFRICHTER

*Laboratory of Chemical Physics, Building 5,
National Institute of Diabetes and Digestive and
Kidney Disease, National Institutes of Health,
Bethesda, Maryland 20892-0520*

Received November 25, 1997

Introduction

Theoretical studies describe protein folding as motion of the polypeptide chain on a partially rough, funnel-shaped energy landscape. This work, beginning with the study of Bryngelson and Wolynes, consists of both analytical theory using concepts of modern statistical mechanics,^{1–3} and computer simulations of simplified representations of proteins.^{2,4} The theoretical studies have had a major impact on the experimental work by emphasizing the statistical nature of the process, and by more clearly defining the important questions for mechanistic investigations. Until a few years ago, kinetic studies of protein folding were limited to studies on time scales of milliseconds or longer, a limitation set by stopped-flow instruments. The theoretical work suggested that much of the kinetics on these time scales resulted from the escape of misfolded or partially folded structures from traps in the energy landscape and not from direct routes to the native which are presumed to occur much more rapidly. This suggestion, together with experimental observations of significant unresolved amplitude in stopped-flow experiments, played a major role in motivating the development of new experimental methods to

study processes on the previously inaccessible submilli-second time scale.

To define the questions that can be addressed by this new generation of “fast” folding experiments, it is instructive to consider an experiment in which refolding of a chemically denatured protein is initiated by sudden dilution of the denaturant (Figure 1). For a protein exhibiting two-state thermodynamic and kinetic behavior, two processes are expected. The first is a collapse of the unfolded polypeptide to more compact denatured structures under the new solvent conditions that favor folding, and the second is crossing the effective free energy barrier from the new denatured state to the native state. How fast is the initial collapse to the more compact denatured structures? How fast do secondary structural elements form, and how is their formation related to the collapse process? What is the height of the free energy barrier separating native and denatured states, and how do we determine it from experimental rate constants? How fast can a protein possibly fold? Does the chain initially collapse to a random distribution of topologies (a “random globule”), as suggested by lattice simulations?⁴ Or does the protein collapse directly to compact structures with topologies similar to that of the native structure but without specific side-chain interactions, as described for the so-called “molten globule?”⁵ The barrier-crossing process should be quite different for random globule and molten globule denatured states. In the former it involves a search for the correct chain topology. In the latter the folding problem at the level of chain topology is “solved” in the initial collapse process, so that barrier crossing involves primarily a reorientation of the side chains in an annealing process.

To address these questions, we and others have developed new ways of more rapidly initiating the folding and unfolding reaction, including photochemical triggering,^{6,7} laser-temperature jump,^{8–10} and ultrarapid mixing.^{11,12} In this account we describe how our development and application of these three rapid kinetic methods has contributed to understanding the dynamics of protein folding. We describe both a “bottom-up” and a “top-down” approach to this problem. In the bottom-up approach, we have investigated the dynamics of three basic elements of protein structure in isolation, loops, α -helices, and β -hairpins. Our experimental results and theoretical modeling lead to a deeper understanding of the mechanism of formation of these structures. They also provide a basis for estimating an upper limit on the rate of protein folding. In the top-down approach we have studied the submillisecond kinetics of a fast-folding protein, cytochrome c. This work has placed limits on the rate of polypeptide collapse, and together with the results on structural elements has also suggested that free energy barrier heights are quite small. Overall, our studies have given the first glimpse of the time scales associated with a number of different fundamental dynamic processes in protein folding.

William A. Eaton received B.A., M.D., and Ph.D. degrees from the University of Pennsylvania. He then joined the National Institutes of Health in 1968, where he is currently Chief of the Laboratory of Chemical Physics and of the Biophysical Chemistry Section.

Victor Muñoz received a Licenciatura from the Autonomous University of Madrid and a Ph.D. from the European Molecular Biology Laboratory, Heidelberg in 1995. He is currently a Fellow of the Human Frontiers Program and Visiting Fellow.

Peggy A. Thompson received a B.S. from Washington State University and a Ph.D. from the University of California, San Diego in 1992. She is currently a Staff Fellow.

Eric R. Henry received B.S. and B.A. degrees from the University of Rochester and a Ph.D. from Princeton University in 1980. He then joined the National Institutes of Health where he is currently a Research Physicist.

James Hofrichter received a B.A. from Dartmouth College and a Ph.D. from the University of Oregon in 1971. He then joined the National Institutes of Health where he is currently Chief of the Laser Biophysics and Spectroscopy Section.

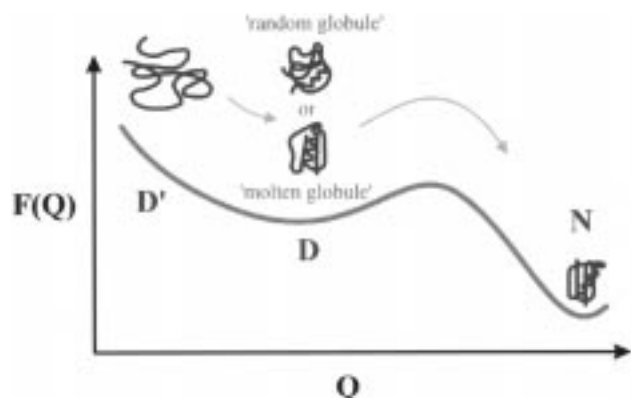


FIGURE 1. Free energy profile for refolding of a two-state protein from the chemically denatured state.

Loop Formation Kinetics

Our studies of “fast” protein folding began with an optical-triggering experiment on a small protein, cytochrome *c*, in the reduced (Fe(II)) state (Figure 2a).⁶ Above ~ 3 M denaturant (GuHCl), carbon monoxide (CO) unfolds cytochrome *c* because the heme in the denatured protein binds CO with a much higher affinity than in the native conformation (Figure 2b). Folding of cytochrome *c* can therefore be initiated by photodissociation, which occurs in less than a picosecond (Figure 2b). Although this optical triggering method dramatically improved the time-resolution of folding experiments, submillisecond folding was not observed. The left shift in the unfolding curve (Figure 2b) produced by CO was simply insufficient to reach the low denaturant concentrations required for submillisecond folding.¹³ We did, however, observe interesting intramolecular ligand binding kinetics in the unfolded molecule that allowed the first investigation of the dynamics of forming a contact between two distant regions of a polypeptide chain, a fundamental process in protein folding.

Following photodissociation of CO, the sixth coordination position is vacant, and the heme iron can now bind histidines and methionines in an intramolecular process. Binding of these ligands is readily observed because they produce characteristic changes in the heme optical spectrum. By kinetic modeling of the nanosecond resolved spectra (Figure 2c) we found that the methionines bind with a time constant of $\sim 40 \mu\text{s}$, which is ~ 10 times faster than the histidines, even though the histidines are much closer in sequence⁶ (Figure 2a). To understand this result we measured the bimolecular binding rate of the free ligands to the heme covalently connected to the 11–21 undecapeptide. In the bimolecular reaction, histidine binds ~ 500 -fold more slowly than methionine, indicating that the chemical barrier to binding is much larger. Methionine binds, moreover, with a nearly diffusion-limited bimolecular rate of $2 \times 10^8 \text{ M}^{-1}\text{s}^{-1}$, indicating that intramolecular methionine binding in the denatured protein is also diffusion limited.¹⁴ This conclusion was made rigorous by a detailed analysis of the two-step mechanism (Figure 3). The final result was that the measured time of $\sim 40 \mu\text{s}$ for intramolecular methionine

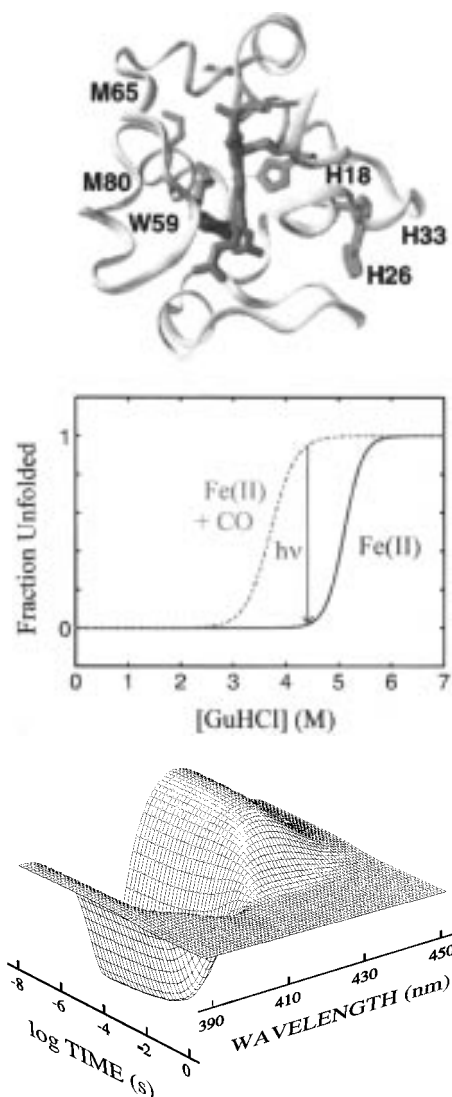


FIGURE 2. Photochemical triggering of reduced cytochrome *c* folding.⁶ (a, top) Key structural features of cytochrome *c*. The heme iron is axially coordinated to methionine 80 (M80) and histidine 18 (H18). In the unfolded (denatured) state H18 remains coordinated, and histidines 26 and 33 and methionines 65 and 80 may bind to the iron. (b, middle) Fraction unfolded (as measured by fluorescence or circular dichroism) versus GuHCl concentration in the presence and absence of carbon monoxide (CO). (c, bottom) Nanosecond-resolved difference absorption spectra following photodissociation of CO.

binding is also the characteristic time for the diffusion-controlled formation of a contact between regions of an unfolded polypeptide separated by ~ 50 residues.¹⁴

Loops in proteins are much shorter than 50 residues long, and we wanted to estimate a rate for the fastest forming loops. Thirumalai and co-workers¹⁵ had developed a theoretical model for a polypeptide chain suggesting that the most probable loops contain ~ 10 residues. Longer loops are less probable because they have lower entropy, and shorter loops are less probable because of chain stiffness. Furthermore, in the simplest theory for loop formation in a polymer by Szabo et al.,^{6,16} the length dependence of the equilibrium constant is contained completely in the formation rate. A 10-residue loop is therefore predicted to be the fastest-forming loop. Using

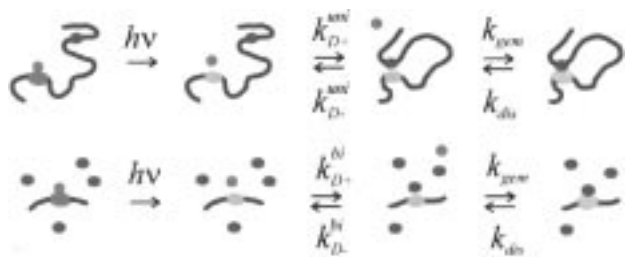


FIGURE 3. Two-step mechanism for unimolecular and bimolecular ligand binding following CO photodissociation.¹⁴ After photodissociation of CO (red) the heme (pink) forms an encounter complex with a histidine or methionine ligand (green). This is followed by either diffusional separation or covalent binding, which is assumed to have the same rate (k_{gem}) in the unimolecular and bimolecular case. The quantity of interest, the diffusion-limited rate to form the encounter complex in the unimolecular case ($k_{D^+}^{\text{uni}}$), can then be obtained from the measured unimolecular and bimolecular rates using a simple analytical expression. The methionine or histidine ligands are eventually displaced from the heme by CO, which has a higher affinity.

our $1/(40 \mu\text{s})$ rate, with either the length scaling for a random coil ($N^{-3/2}$) or the scaling of the loop probability from the Thirumalai theory, produces a rate for the fastest-forming loop of $\sim 10^6 \text{ s}^{-1}$. This is a rough estimate not only because of the approximations involved in the scaling, but also because the dynamical properties of loops should be composition dependent,¹⁷ an important subject for future investigations.

α -Helix Formation: Generalization of a “Kinetic Zipper” Model

The loop study relied on very specific chemistry that is unique to heme proteins. We were interested in developing more generic methods to study fast-folding processes. As did several other research groups,^{8,9} we developed a laser temperature jump apparatus.^{10,18} Heating is carried out with a Q-switched Nd:YAG laser with a fundamental at 1064 nm, which is Raman shifted to 1540 nm by a methane-containing high-pressure cell. At this wavelength vibrational overtones of the water O–H stretch are excited, thereby directly heating the solvent with a rise time close to the $\sim 5 \text{ ns}$ laser pulse width. With an illumination volume of $\sim 10^{-4} \text{ cm}^3$, temperature jumps of 20° can be maintained for several milliseconds, giving a temporal dynamic range of almost 10^6 . The probe source is either a visible or ultraviolet cw laser that can be used for absorption or fluorescence measurements.

As a “warm-up” for studying protein folding and a test of our new instrument we investigated the helix–coil transition kinetics of an alanine-based peptide previously studied by time-resolved infrared (IR) spectroscopy.⁹ The peptide we studied differed only in the attachment of methyl amino benzoic acid (MABA) at the N-terminus. NMR studies had suggested that increased MABA fluorescence is an indicator of helix formation.¹⁹ Following a temperature jump we found a single-exponential relaxation at $\sim 20 \text{ ns}$ for the probe fluorescence, which is ~ 10 times faster than the relaxation for the average helix

content observed by IR spectroscopy.⁹ We also found that the fluorescence relaxation rate is almost temperature independent (only a single temperature was investigated in the IR study⁹). These results were puzzling, and as happens frequently in research, what started out as a quick test became a full-blown project.

To interpret these data we first explored the simplest possible model, treating the peptide as homopolymer.¹⁰ We called it the “kinetic zipper” model because it is the kinetic analogue of the classic equilibrium “zipper” model in which molecules contain either no helix or a single stretch of helix. In this model, residue i is either in a coil state (c) or a helix state (h), the latter defined by the formation of a hydrogen bond between its backbone carbonyl O and the NH of residue $i + 4$ in the sequence. A key simplification is the single sequence approximation of Schellman,²⁰ which assumes that nucleation of the helix is sufficiently improbable that it occurs only once in each molecule. That is, species such as $..cchhhhccc..$ are populated, but not $..cchhcchhcc..$. Each kinetic species is therefore defined by just two variables, the first residue in the helix and the total number of helical residues. Once nucleated, the helix grows (“zips up”) by adding residues at either end. The single sequence approximation reduces the number of species from 2^n to $n(n + 1)/2 + 1$ for a peptide that forms a maximum of n hydrogen bonds ($n + 4$ residues).

Numerical solution of the differential equations describing the model predicted that for the average helix content most of the amplitude occurs in a single exponential phase, as observed in the IR study.¹⁰ Breakage and reformation of the hydrogen bond of the N -terminal residue, on the other hand, was predicted to exhibit approximately biexponential kinetics with roughly equal amplitudes, the faster relaxation corresponding to rapid redistribution of helical lengths, the slower from crossing the nucleation barrier (with the same $\sim 1/(200 \text{ ns})$ rate as the average helix content). In contrast, the experiment showed a single fast ($\sim 20 \text{ ns}$) exponential relaxation. This discrepancy was difficult to understand. Was the simple kinetic description of nucleation and growth of a single stretch of helix incorrect or was the MABA probe not a faithful measure of helix formation?

To investigate this question we studied a similar peptide without the MABA probe. In this peptide the first residue (alanine) was replaced by tryptophan and the fifth (also alanine) was replaced by histidine (Figure 4a).²¹ Tryptophan fluorescence was expected to probe α -helix formation because the side chains of residues i and $i + 4$ interact in an α -helix, and histidine efficiently quenches tryptophan fluorescence when it is protonated.²² With this peptide we found that the fluorescence changes are much slower and temperature dependent, with a single relaxation time of 220 ns at 27°C , about the same time observed for the peptide of the IR study⁹ (Figure 5).

Again, a probe at the N-terminus is not exhibiting biphasic kinetics. How do we explain this? We reasoned that a homopolymer model could no longer be used to analyze these data because the propensity of both trypt-

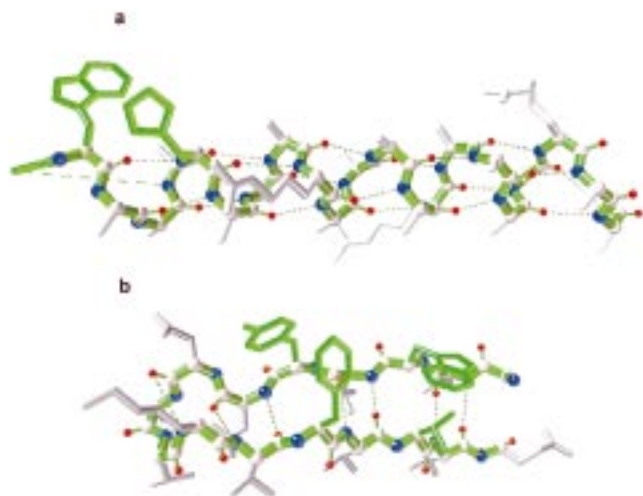
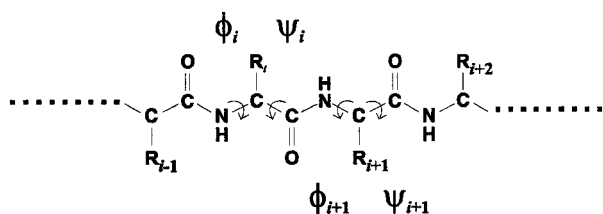


FIGURE 4. Structure of α -helix and β -hairpin used in T-jump studies. (a) Helix-forming peptide Ac-WAAAAH(AAARA)₃A-NH₂. The N-terminus is acetylated and the C-terminus is amidated. (b) Hairpin forming peptide GEWTYDDATKTFTVTE.

tryptophan and histidine to adopt a helical backbone conformation is known from a comprehensive analysis of equilibrium studies to be much less than that of alanine and arginine (which are about equal).²³ Furthermore, significant side-chain interactions have been introduced in this peptide which must also be taken into account. We therefore required a model that could readily treat both heteropeptides and side-chain interactions, and turned to the same model that Muñoz and co-workers had successfully employed in describing the β -hairpin-forming peptide discussed below.^{24,25} This model classifies structures according to the backbone conformation. A conformation is defined by the set of values of the dihedral angle pairs (ψ of residue i and ϕ of residue $i + 1$) corresponding to each CONH peptide bond. Each pair determines the orientation of the C _{α} -C _{β} bonds of adjacent residues in the sequence, which is convenient for treating side-chain interactions.



Two states are considered for each peptide bond – native (i.e., helical dihedral angles for ψ_i and ϕ_{i+1}) and non-native (i.e., nonhelical values for one or both ψ_i and ϕ_{i+1}). There are therefore 2^n possible conformations for a peptide containing $n + 1$ residues. For our 21-residue peptide the single sequence approximation reduces the number of conformations from over 4 million to 254. A major simplification in the model is that interactions between two groups (i.e., backbone hydrogen bonds or side-chain interactions) occur only if all intervening peptide bonds have native values. A hydrogen bond between the CO of residue i and the NH of residue $i + 4$ forms when the four

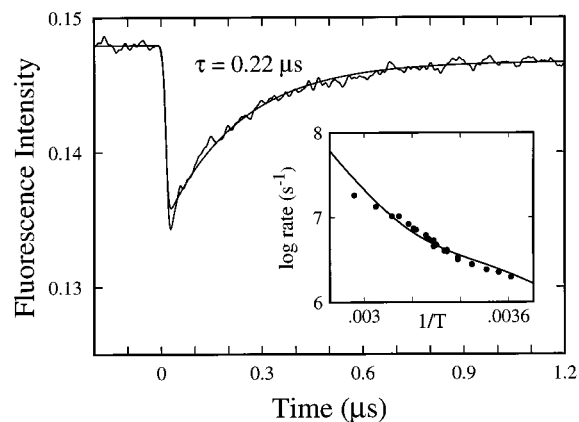


FIGURE 5. Helix–coil kinetics.²¹ Kinetic trace following a temperature jump from 289 to 300 K with single exponential fit. The initial decrease follows the laser pulse and is due solely to the intrinsic temperature dependence of tryptophan fluorescence. (insert) Relaxation rates (points) as a function of temperature with theoretical curves from statistical mechanical model.

intervening peptide bonds are in the helical conformation. Similarly the indole side chain of tryptophan forms a stabilizing interaction with the protonated imidazole side chain of histidine when the four intervening dihedral angle pairs have helical values. There is also a repulsive interaction between the protonated histidine and the positively charged arginine in the $i + 4$ position upon helix formation. The thermodynamic factors included in the model are thus the stabilizing CO \cdots HN backbone hydrogen bonds, a stabilizing and a destabilizing side-chain interaction, and the destabilizing entropy change upon fixing a ψ_i, ϕ_{i+1} pair in a helical conformation (used as a measure of helix propensity, one value for alanine and arginine and another for tryptophan and histidine²³).

This model predicts all of the major features of the tryptophan fluorescence kinetics, while simultaneously fitting both the circular dichroism and fluorescence equilibrium melting curves.²¹ Because of the strong interaction between tryptophan and histidine, there is little fraying at the N-terminus. The fraction of helix at the N-terminus therefore closely parallels the average helix content, and the predicted kinetics are dominated by a single exponential relaxation, as observed experimentally (Figure 5), with a rate close to that of the average helix content. The model also predicts a fast relaxation associated with the redistribution of helical lengths, but this would not be resolved with our instrument because of its very small amplitude (<5%) and speed ($\tau = 1$ –10 ns). Simulation of the kinetics of a homopolymer with this model reproduces the behavior observed with the simpler kinetic zipper model. In particular, it predicts approximately biexponential kinetics with similar amplitudes for the N-terminal helical turn.²¹ The apparent failure of MABA fluorescence to faithfully monitor helix formation thus remains to be explained.

The success of the model suggests that the basic picture of nucleation and growth of a single stretch of helical residues is still a viable mechanism. It also suggests that it will be possible to understand the kinetics of even more

complex heteropeptides, as has been done in equilibrium studies,²⁶ using the tryptophan–histidine pair as a probe. It will be interesting to not only vary the position of this pair, but also to investigate the length and composition dependence of the kinetics.

Statistical Thermodynamics and Kinetics of a β -Hairpin

Having invested a significant effort in studying the dynamics of loops and helices, it seemed only natural to investigate β -structure, the other common secondary structure in proteins. We chose to study a β -hairpin, the basic element of the antiparallel pleated sheet and the simplest β -structure (Figure 4b). It is perhaps surprising that prior to our work there were no experimental thermodynamic or kinetic studies of isolated β -structure formation. Isolated β -hairpins appear to require hydrophobic interactions between side chains for stability, so that either one or both faces of the structure are sticky, making them prone to aggregation. However, several monomeric peptides have recently been shown to exhibit β -hairpin structure. We have studied one such peptide, the 16-residue C-terminal fragment of protein G B1 (Figure 4b).^{24,25} The β -hairpin conformation of this peptide contains a hydrophobic cluster consisting of a tyrosine, phenylalanine, valine, and a tryptophan.²⁷ The tryptophan was used to probe hairpin formation in two ways. First the intrinsic tryptophan fluorescence was monitored. Upon forming a hydrophobic interaction with the valine and phenylalanine, the fluorescence increases because of decreased water exposure and therefore less solvent quenching. Because fluorescence quenching is still not completely understood, we wanted another fluorescent probe, so a dansylated lysine was added to the C-terminus of the peptide. The dansyl absorption strongly overlaps the tryptophan fluorescence, and quenches its fluorescence as an acceptor of excitation energy via a transition dipole–dipole (Forster) coupling mechanism. In this case, the change in fluorescence is dominated by the Forster mechanism, and upon unfolding there is a net increase in fluorescence from the increased average distance between the tryptophan and dansyl groups.

The results turned out to be remarkably clear and straightforward to interpret.^{24,25} The equilibrium thermal unfolding curve of both the dansylated and undansylated β -hairpin could be accurately described by a two-state model. The kinetics following the temperature jump are described by a single-exponential relaxation, with the same relaxation time of 3.5 μ s for the dansylated and undansylated peptide (Figure 6). The finding of a single exponential with the same relaxation rate using essentially independent probes is characteristic of two-state kinetic behavior. A two-state analysis of the equilibrium and kinetic data indicated that the β -hairpin folds with an apparent *negative* activation energy of ~ 1 kcal/mol. (The relaxation rate, which is the sum of the folding and unfolding rates, increases with increasing temperature because of the positive and larger activation energy of the

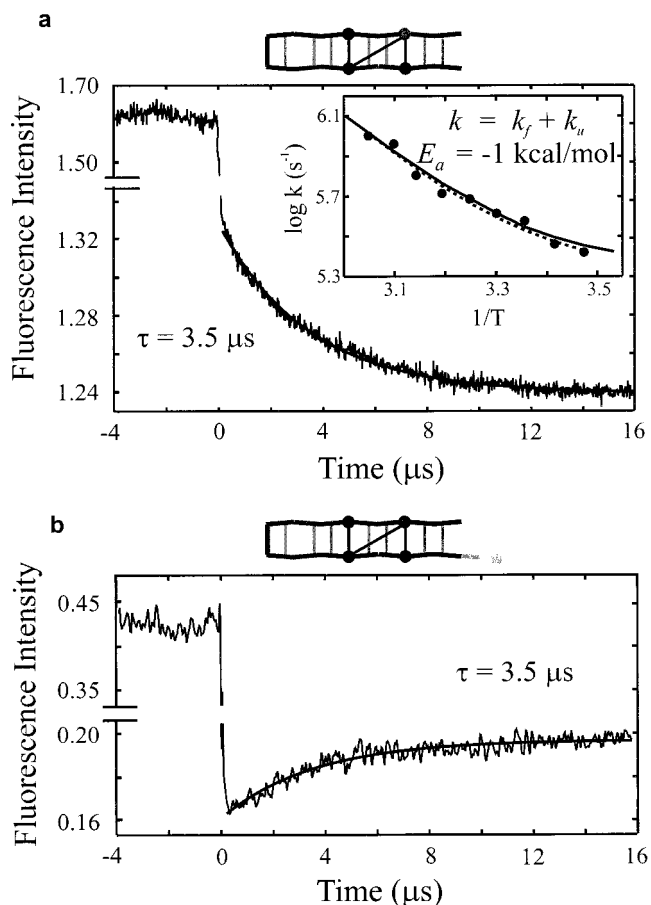


FIGURE 6. Kinetics of β -hairpin unfolding/refolding with exponential fit.²⁴ (a) Tryptophan fluorescence following a T-jump from 273 to 288 K with Arrhenius plot of relaxation rate as inset (the red curve is from a two-state model and the blue curve is from the statistical mechanical model); (b) same experiment on dansylated peptide.

unfolding rate.) In a two-state analysis, the β -hairpin folding rate at the T_m is ~ 6 μ s, more than 10-fold slower than the rates determined for α -helix formation.

To explain the three basic experimental facts for folding of a β -hairpin – two-state behavior, an apparent negative activation energy, and slower-than- α -helix kinetics – we applied the statistical mechanical model already described for the helix.^{24,25} As with the helix, each peptide bond can exist in two states – native and non-native. In this case, however, native refers to either a strand conformation or a turn conformation. Again, non-native (side-chain and hydrogen-bond) interactions are not considered, and native interactions only occur when all intervening dihedral angle pairs have native values. The single sequence approximation was also employed for the β -hairpin, and reduces the number of species from 2^{15} for this 16-residue peptide to 121. This approximation was shown to be valid in kinetic simulations in which the 2^{15} differential equations were solved.²⁵ In a manner similar to the α -helix, each kinetic species is defined by two variables – the number of contiguous native peptide bonds and the location of the central peptide bond in the contiguous segment, resulting in a two-dimensional free energy surface.

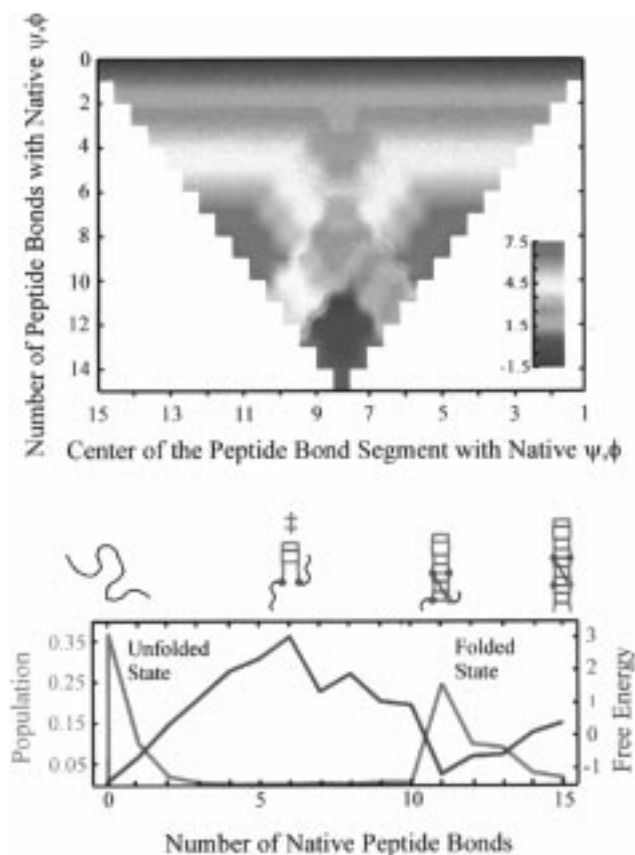


FIGURE 7. Free energy surface and profile for β -hairpin-forming-peptide calculated from statistical mechanical model.^{24,25}

This surface, which was calculated using the parameters that simultaneously fit the equilibrium and kinetic data, shows that there are two global minima, one for the unfolded hairpin, and another for the folded hairpin. The most stable β -hairpin structure is one with all hydrophobic interactions intact, but without two hydrogen bonds connecting the N and C terminal parts of the chain. The global minima are separated by a significant barrier, immediately explaining the two-state kinetic and equilibrium behavior. At the top of this barrier, the (yellow) saddle point on the pass between the (red) mountains is the transition state in which the peptide has two hydrogen bonds, but no hydrophobic side-chain interactions (Figure 7). This transition state is therefore at a *lower energy* than the unfolded state by ~ 1 kcal/mol, explaining the apparent negative activation energy for folding in the two-state analysis.

The model also explains the slower formation rate for the β -hairpin compared with the α -helix. The helix can nucleate (i.e., cross the free energy barrier between the all-coil state and helical states) at any one of 12 positions for a 16-residue peptide. In contrast, the β -hairpin can only reach the top of the barrier by forming the central turn region. Moreover, once the first hydrogen bond is formed in the helix, growth is downhill in free energy because the stabilization energy of forming a single hydrogen bond is sufficient to overcome the destabilizing effect of fixing a single dihedral angle pair in the helical

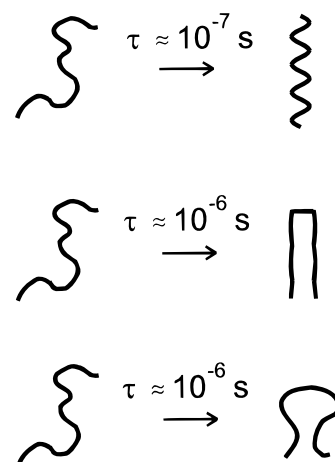


FIGURE 8. Time scales for the formation of an α -helix, a β -hairpin, and a 10-residue loop.

conformation. Growth of a β -hairpin is uphill in free energy in the absence of stabilizing side-chain interactions because the entropy loss in fixing two peptide bonds (two ψ_i, ϕ_{i+1} pairs) in their native conformation to form a single hydrogen bond is greater than the hydrogen bond energy. The net result of these two factors is that the free energy barrier to hairpin formation is greater. Similar relative and absolute times for α -helices and β -hairpins have been obtained by Klimov and Thirumalai²⁸ in Langevin dynamics studies of simplified representations, suggesting that such simulations can be extremely useful in investigating structural aspects of the mechanism.

Despite the success of the model in describing both helices and hairpins, one could envisage other mechanisms for the hairpin, such as loop formation to form a hydrophobic cluster (“hydrophobic collapse”) followed by rapid formation of hydrogen bonds. This possibility can be tested by repositioning the cluster closer or farther away from the turn such that the resulting loop may be either shorter or longer than the loop length at the Thirumalai maximum discussed earlier. Similar issues have been raised for protein folding. Indeed one of the surprises exposed by our analysis is that β -hairpin formation of a peptide containing only 16 residues captures much of the basic physics of protein folding.^{1–4,29}

A “Speed Limit” for Protein Folding and Dynamics of a Fast-Folding Protein

How fast can a protein possibly fold? At low denaturant concentration, time constants of ~ 1 – 20 ms have been measured for small proteins.³⁰ At zero denaturant concentration these proteins may fold much faster, with extrapolated values as small as ~ 70 μ s.³¹ Our results on structural elements provide an estimate of a “speed limit.” The data so far indicate that helices form in $\sim 10^{-7}$ s, small loops and hairpins in $\sim 10^{-6}$ s (Figure 8). Thus, for both α -helical and β -sheet proteins, the slowest forming structural element requires ~ 1 μ s, and therefore may be taken as an empirical estimate for the shortest time in which a protein can possibly fold. This rate of 10^6 s^{-1} might be

regarded as the unimolecular equivalent for proteins of the Smoluchowski limit for diffusion-controlled bimolecular reactions in solution. What is lacking in the protein case, however, is a comparable theoretical analysis, although there are now efforts in that direction.³²

These considerations suggested that it would be worthwhile to try to improve the time-resolution of mixing experiments to measure the fastest folding kinetics. Our interest in this approach was sparked after learning from D. L. Rousseau of a new continuous flow methodology for mixing solutions in a few microseconds, a technique originally developed by Regenfuss et al.³³ to study a very fast bimolecular reaction. The basic idea of the method is that the turbulence created by forcing liquids at a high velocity through a small gap effectively "breaks" the liquids into small pieces, called turbulent eddies. The dimension over which the solutes must diffuse to mix is now the size of these eddies, which can be $<0.1 \mu\text{m}$, producing diffusion times of $<10 \mu\text{s}$. Spectral measurements are made at a series of positions along the freely flowing jet that emerges from the mixer. Since each position corresponds to a time after mixing, this yields a kinetic trace.^{11,12,33}

With this new method we first measured the submillisecond folding kinetics of cytochrome c following dilution of guanidinium chloride.¹¹ There is a large unresolved amplitude in stopped flow experiments when cytochrome c is refolded from guanidine-denatured solutions.^{34,35} Cytochrome c therefore seemed to be a good test case for this new methodology. To eliminate intramolecular binding of ligands and the associated formation of misfolded structures,^{12,34,35} we studied the imidazole complex of cytochrome c.¹¹ The results were striking (Figure 9). The decrease in fluorescence of the lone tryptophan 59 (Figure 2a) which is due to Forster quenching as the distance to the heme decreases, is markedly biphasic. There is an immediate drop in fluorescence that could not be resolved with the $70\text{-}\mu\text{s}$ dead time of our instrument, indicating $\tau < \sim 50 \mu\text{s}$. This is followed by a single-exponential relaxation with $\tau \approx 600 \mu\text{s}$ at the lowest denaturant concentration studied (0.25 M GuHCl). In this experiment, folding is essentially complete before any observations could be made by conventional stopped-flow techniques.

There is a straightforward interpretation to these results. The sub- $50\text{-}\mu\text{s}$ process corresponds to partial collapse of the polypeptide chain to form more compact denatured structures, whereas the resolved exponential process corresponds to the barrier crossing to the native conformation (Figure 1). The fluorescence of the denatured state drops sharply as the final denaturant approaches zero, in agreement with the expectation that it becomes more compact.^{34,35}

These results bring us back to fundamental issues of folding dynamics raised in the Introduction to this paper. We did not resolve collapse, but did set an upper limit of $\sim 50 \mu\text{s}$.³⁶⁻³⁸ We also set an upper limit on the height of the free energy barrier separating the native and denatured state (Figure 1). Assuming that the folding rate constant has the form $k_o \exp(-\Delta G^\ddagger/RT)$, then the preex-

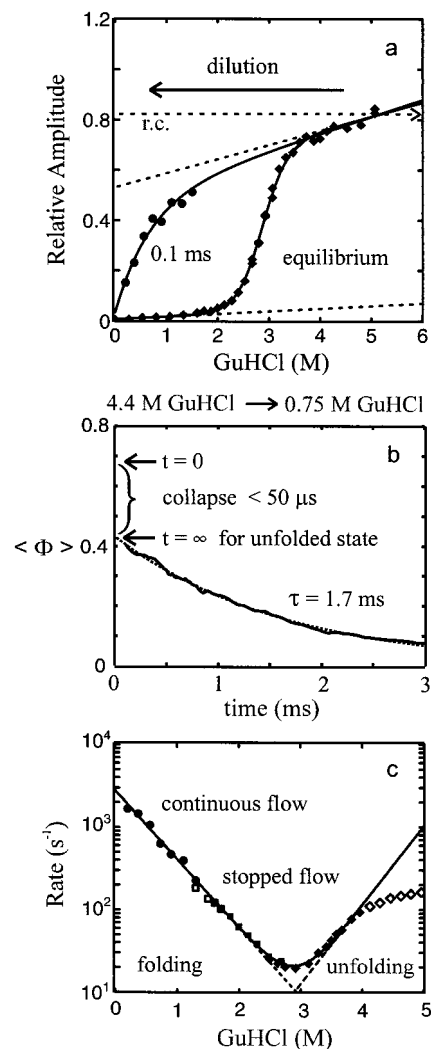


FIGURE 9. Kinetics of refolding imidazole cytochrome c after ultrarapid dilution of guanidinium chloride.¹¹ (a) Equilibrium unfolding curve (diamonds) and fluorescence amplitudes at $100 \mu\text{s}$ after dilution (circles). Horizontal dashed line labeled r.c. is calculated fluorescence for random coil from Forster theory, (b) kinetic progress curve with exponential fit showing unresolved partial collapse, (c) rate versus final GuHCl concentration from continuous flow (circles) and stopped flow (squares and diamonds) experiments.

ponential factor k_o would be the rate constant for folding in the absence of a barrier ($\Delta G^\ddagger = 0$) ($k_o = k_B T/h = 6 \times 10^{12} \text{ s}^{-1}$ from transition state theory obviously does not apply to protein folding). We expect this rate to correspond to the fastest that a protein could possibly fold, because it is a process that is continuously downhill in free energy – “scenario 0” in the classification of Wolynes and co-workers.^{2,39} Thus, our value of 10^6 s^{-1} is also a tentative estimate for an *upper limit* for the preexponential factor; using the maximum observed rate of $1/(600 \mu\text{s})$ places an upper limit on the height of the free energy barrier of $\sim 4 \text{ kcal/mol}$ for cytochrome c. This low value is interesting for two reasons. First it supports theoretical studies that suggest barriers to fast-folding small proteins are quite small.⁴⁰ Second, it suggests that it might be possible to either manipulate solution conditions or mutate the protein to eliminate the barrier. In a two-state

system, only the unfolded state and native state can be directly observed. The thermodynamic properties of the transition state ensemble can be obtained by the site-directed mutagenesis approach of Fersht,⁴¹ from which structural inferences are made. The importance of the downhill scenario is that intermediate structures between the unfolded and native states could become significantly populated, allowing, in principle, spectroscopic observation of the complete evolution of the structure distribution as a protein folds.

Biological Significance and Future Directions

A new idea emerging from the theoretical studies is that kinetic foldability as well as functionality might be a selective pressure in evolution.² Fast-folding experiments have raised the question: how quickly *must* a protein fold? What may be most critical is that the nascent polypeptide released from the ribosomes or chaperonins be able to avoid aggregation by rapidly forming compact structures that do not expose sticky hydrophobic patches on the molecular surface. Final rearrangement to the native, biologically functional conformation could be much slower depending on the requirements of the cell. Our question should therefore be rephrased: how fast must compact structures with maximal burial of hydrophobic residues be formed? These considerations suggest that understanding the fast processes in protein folding may be biologically more important than the slower processes, which have been the subject of most kinetic investigations up to now.

Fast-folding studies are clearly in their infancy with limited experimental data. However, the results obtained so far raise many new and interesting questions that can be approached by experimental kinetics. Our studies of loops, α -helices, and β -hairpins suggest that it should be possible to investigate the kinetics of folding using an "aufbau" approach, in which increasingly complex structures made from combinations of structural elements are studied experimentally and modeled in detail. Also, computing power is rapidly reaching a level where very long, all-atom molecular dynamics trajectories will be calculated that overlap the time scale of these experiments. Such simulations will be an important guide in the further development of kinetic models. Finally, there are also prospects of performing single-molecule folding experiments. These studies are important because the ultimate experimental description of protein folding is one of determining the time-dependent distribution of structures as the system proceeds from the myriad of unfolded conformations to the unique native structure.

We thank Peter Wolynes for motivating this research by pointing out the importance of fast-folding kinetics. We also thank Peter Wolynes, Attila Szabo, Dev Thirumalai, and Robert Zwanzig for many helpful discussions on theoretical issues.

References

- (1) Bryngelson, J. D.; Wolynes, P. G. *Proc. Natl. Acad. Sci. U.S.A.* **1987**, *84*, 7524–7528.

- (2) Bryngelson J. D.; Onuchic J. N.; Socci N. D.; Wolynes P. G. *Proteins: Struct. Funct., Genet.* **1995**, *21*, 167–195.
- (3) Orland, H.; Garel, T.; Thirumalai, D. T. In *Recent Developments in Theoretical Studies of Proteins*; Elber, R., Ed.; World Scientific: Singapore, 1996; pp 197–268.
- (4) Dill, K. A.; Bromberg, S.; Yue, K.; Feibig, K. M.; Yee, D. P.; Thomas, P. D.; Chan H. S. *Prot. Sci.* **1995**, *4*, 561–602; Karplus, M.; Sali, A. *Curr. Opin. Struct. Biol.* **1995**, *5*, 58–73; Thirumalai, D.; Woodson, S. A.; *Acc. Chem. Res.* **1996**, *29*, 433–439; Shakhnovich, E. I. *Curr. Opin. Struct. Biol.* **1997**, *7*, 29–40.
- (5) Ptitsyn, O. B. *Adv. Prot. Chem.* **1995**, *47*, 83–225.
- (6) Jones, C. M.; Henry, E. R.; Hu, Y.; Chan, C.-K.; Luck, S. D.; Bhuyan, A.; Roder, H.; Hofrichter, J.; Eaton, W. A. *Proc. Natl. Acad. Sci. U.S.A.* **1993**, *90*, 1860–11864.
- (7) Pascher, T.; Chesick, J. P.; Winkler, J. R.; Gray, H. B. *Science* **1996**, *271*, 1558–1560; Telford, J. R.; Wittung-Stafshede, P.; Gray, H. B.; Winkler, J. R. *Acc. Chem. Res.* **1998**, *31*, 755–763.
- (8) Phillips, C. M.; Mizutani, Y.; Hochstrasser, R. M. *Proc. Natl. Acad. Sci. U.S.A.* **1995**, *92*, 7292–7296; Nolting, B.; Golbik, R.; Fersht, A. R. *Proc. Natl. Acad. Sci. U.S.A.* **1995**, *92*, 10668–10672; Ballew, R. M.; Sabelko, J.; Gruebele, M. *Proc. Natl. Acad. Sci. U.S.A.* **1996**, *93*, 5759–5764; Gruebele, M.; Sabelko, J.; Ballew, R.; Ervin, J. *Acc. Chem. Res.* **1998**, *31*, 699–707.
- (9) Williams, K.; Causgrove, T. P.; Gilmanishin, R.; Fang, K. S.; Callender, R. H.; Woodruff, W. H.; Dyer, R. B. *Biochemistry* **1996**, *35*, 691–697; Dyer, R. B.; Gai, F.; Woodruff, W. H.; Gilmanishin, R.; Callender, H. *Acc. Chem. Res.* **1998**, *31*, 709–716.
- (10) Thompson, P. A.; Eaton, W. A.; Hofrichter, J. *Biochemistry* **1997**, *36*, 9200–9210.
- (11) Chan, C. K.; Hu, Y.; Takahashi, S.; Rousseau, D. L.; Eaton, W. A.; Hofrichter, J. *Proc. Natl. Acad. Sci. U.S.A.* **1997**, *94*, 1779–1784.
- (12) Takahashi, S.; Yeh, S. R.; Das, T. K.; Chan, C. K.; Gottfried, D. S.; Rousseau, D. L. *Nat. Struct. Biol.* **1997**, *4*, 44–50; Yeh, S.-R.; Han, S.; Rousseau, D. L. *Acc. Chem. Res.* **1998**, *31*, 727–736.
- (13) A larger difference in stability and consequent faster folding has been achieved by Gray and co-workers⁷ using a conceptually similar method in which folding is initiated by the optically triggered reduction of the ferric state.
- (14) Hagen, S. J.; Hofrichter, J.; Szabo, A.; Eaton, W. A. *Proc. Natl. Acad. Sci. U.S.A.* **1996**, *93*, 11615–11617; Hagen, S. J.; Hofrichter, J.; Eaton, W. A. *J. Phys. Chem.* **1996**, *100*, 12008–12021.
- (15) Guo, Z.; Thirumalai, D. *Biopolymers* **1995**, *36*, 83–102; Camacho, J.; Thirumalai, D. *Proc. Natl. Acad. Sci. U.S.A.* **1995**, *92*, 1277–1281.
- (16) Szabo, A.; Schulten, K.; Schulten, Z. *J. Chem. Phys.* **1980**, *72*, 4350–4357.
- (17) The effective diffusion constant for the heme-methionine motion of $\sim 5 \times 10^{-7} \text{ cm}^2 \text{ s}^{-1}$ calculated from the theory of Szabo et al.¹⁶ agrees well with the value obtained in energy transfer experiments on peptides (Gottfried, D. S.; Haas, E. *Biochemistry* **1992**, *31*, 12353), suggesting that the loop of cytochrome c is not an anomalous one.
- (18) Thompson, P. A. In *Techniques in Protein Chemistry*; Marshak, D. R., Ed.; Academic Press: San Diego, **1997**, pp 735–743.
- (19) Lockhart, D. J.; Kim, P. S. *Science* **1992**, *257*, 947–951.
- (20) Schellman, J. A. *J. Phys. Chem.* **1958**, *62*, 1485–1494.

- (21) Thompson, P. A.; Muñoz, V.; Henry, E. R.; Eaton, W. A.; Hofrichter, J., submitted for publication in *J. Phys. Chem.*
- (22) Steiner, R. F.; Kirby, E. P. *J. Phys. Chem.* **1969**, *73*, 4130–4135.
- (23) Muñoz, V.; Serrano, L. *J. Mol. Biol.* **1995**, *245*, 275–296.
- (24) Muñoz, V.; Thompson, P. A.; Hofrichter, J.; Eaton, W. A. *Nature* **1997**, *390*, 196–199.
- (25) Muñoz, V.; Henry, E. R.; Hofrichter, J.; Eaton, W. A. *Proc. Natl. Acad. Sci. U.S.A.* **1998**, *95*, 5872–5879.
- (26) Chakrabarty, A.; Baldwin, R. L. *Adv. Prot. Chem.* **1995**, *46*, 141–176. Muñoz, V.; Serrano, L. *Curr. Opin. Biotech.* **1995**, *6*, 382–386.
- (27) Blanco, F. J.; Rivas, G.; Serrano, L. *Nature Struct. Biol.* **1994**, *1*, 584–590.
- (28) Klimov, D. K.; Thirumalai, D. *Phys. Rev. Lett.* **1997**, *79*, 317–320.
- (29) Zwanzig, R. *Proc. Natl. Acad. Sci. U.S.A.* **1995**, *92*, 9801–9804.
- (30) See refs 9–15 in Eaton, W. A.; Muñoz, V.; Thompson, P. A.; Chan, C.-K.; Hofrichter, J. *Curr. Opin. Struct. Biol.* **1997**, *7*, 10–14.
- (31) Robinson, C. R.; Sauer, R. T. *Biochemistry* **1996**, *35*, 13878–13884.
- (32) Pitard, E.; Garel, T.; Orland, H. *Europhys. Lett.* **1998**, *41*, 167–172.
- (33) Regenfuss, P.; Clegg, R. M.; Fulwyler, M. J.; Barantes, F. J.; Jovin, T. M. *Rev. Sci. Instrum.* **1985**, *56*, 283–290.
- (34) Ramachandra Shastry, M. C.; Sauder, J. M.; Roder, H. *Acc. Chem. Res.* **1998**, *31*, 717–725.
- (35) Englander, S. W.; Sosnick, T. R.; Mayne, L. C.; Shtilerman, M.; Qi, P. X.; Bai, Y. *Acc. Chem. Res.* **1998**, *31*, 737–744.
- (36) An improved mixer with a shorter dead time (45 μ s) has recently been developed by Roder and co-workers, which permits resolution of this process (*Acc. Chem. Res.* **1998**, *31*, 717–725). Shastry, MCR; Roder, H. *Nat. Struct. Biol.* **1998**, *5*, 385–392.
- (37) The suggestion from absorption experiments that the cytochrome c collapses after optically triggered folding at $\sim 40 \mu$ s was not supported by excitation energy transfer measurements with nanosecond time-resolution (Chan C.-K.; Hofrichter J.; Eaton W. A. *Science* **1996**, *274*, 628–629).
- (38) See article by Gruebele et al. in this issue for discussion of collapse in apomyoglobin.
- (39) Onuchic, J.; Luthey-Schulten, A.; Wolynes, P. G. *Annu. Rev. Phys. Chem.* **1997**, *48*, 545–600.
- (40) Plotkin, S.; Wang, J.; Wolynes, P. G. *J. Chem. Phys.* **1997**, *106*, 2932–2948.
- (41) Fersht, A. R. *Curr. Opin. Struct. Biol.* **1997**, *7*, 3–9; Onuchic, J.; Socci, N. D.; Luthey-Schulten, A.; Wolynes, P. G. *Folding & Design* **1996**, *1*, 441–450.

AR9700825